Simultaneous trapping of Cr(III) and organic dyes by a pH-responsive resin containing zwitterionic aminomethylphosphonate ligands and hydrophobic pendants

Shaikh A. Ali, Ihsan B. Rachman, Tawfik A. Saleh

PII: S1385-8947(17)31343-8
DOI: http://dx.doi.org/10.1016/j.cej.2017.08.003
Reference: CEJ 17454

To appear in: *Chemical Engineering Journal*

Received Date: 14 June 2017
Revised Date: 31 July 2017
Accepted Date: 1 August 2017

Please cite this article as: S.A. Ali, I.B. Rachman, T.A. Saleh, Simultaneous trapping of Cr(III) and organic dyes by a pH-responsive resin containing zwitterionic aminomethylphosphonate ligands and hydrophobic pendants, *Chemical Engineering Journal* (2017), doi: http://dx.doi.org/10.1016/j.cej.2017.08.003

Simultaneous trapping of Cr(III) and organic dyes by a pH-responsive resin containing zwitterionic aminomethylphosphonate ligands and hydrophobic pendants

Shaikh A. Ali*, Ihsan B. Rachman, and Tawfik A. Saleh

Department of Chemistry, King Fahd University of Petroleum & Minerals, Dhahran 31261, Saudi Arabia

*Corresponding author

E-mail address: shaikh@kfupm.edu.sa

Tel.: (966)13 860 7836; Fax: (966) 13 860 4277

Home Page: http://faculty.kfupm.edu.sa/CHEM/shaikh/

ABSTRACT

A novel functionalized resin containing hydrophilic motifs of aminomethylphosphonate and hydrophobic pendant of 6-(biphenyl-4-yloxy)hexyl has been synthesized. The resin has been utilized as a sorbent for the simultaneous removal of Cr(III) as well as several organic dyes from aqueous solutions. At an initial Cr(III) concentration of 1.0 ppm, the metal uptake was almost ≈100% in 20 min at pH 5 and 25 °C. The experimental results were evaluated by Langmuir, Freundlich, and Temkin isotherm models. By using 0.1 M HNO_3 solution, the adsorbed Cr(III) ions were desorbed effectively. Interestingly, the resin demonstrated remarkable efficacy in simultaneous and complete removal of Cr(III) and several dyes including methyl orange, eriochrome black T, rhodamine B, methyl red and methylene blue from their mixture. The resin has also been remarkably effective in the removal of several toxic metal ions from a real industrial wastewater. As such, the resin may have applications for international environmental management in the water technology.

Keywords:

Organic contaminants;
Cross-linked polyzwitterion;
Sorption;
Dye and Cr(III) removal;
Chelating resin

1. Introduction

The presence and toxic effect of pollutants in water bodies have been identified as a global challenge [1,2]. The presence of pollutants in the environment can be attributed to both natural and anthropogenic sources [3]. Heavy metal ions (HMI) are non-biodegradable pollutants accumulated in groundwater and on the soil surface as a waste of some industrial processes such as mining, painting, and anti-corrosive coating. HMI over the normal limit can cause a variety of diseases, which include loss of memory, kidney and renal problems, diarrhea, as well as reproductive disorders. The presence of the metal contaminants may lead to neurological disorder, damage to both respiratory and cardiovascular organs, skin diseases and cancer [4]. The contaminants are also known to biomagnify in organisms thereby increasing their toxic effects as they move up the food chain [5,6]. According to the Environmental Protection Agency, the maximum level of the contaminant of chromium, one of the most dangerous metal ions, in drinking water is 0.1 $mg \bullet L^{-1}$.

To overcome the problems caused by pollutants, more efforts are required to minimize their impact on the environment. Different removal methods have been adopted in the treatment of Cr(III)-contaminated waters that include nanofiltration [7], lime-softening [8], adsorption, reverse osmosis, coagulation [9], electrocoagulation [10], ion exchange, chemical precipitation, etc [11]. Adsorption is considered a promising method relying on the efficiency of water-insoluble/swellable solid sorbent materials.

Designing an appropriate and efficient adsorbent for specific pollutants is the key step for a successful adsorption process. For metal removal from wastewater, conventional adsorbents like clay activated carbon and nanomaterials are used. Inexpensive biodegradable natural polymers

such as cellulose, chitosan and starch are also used because of their abundance, high efficiency, non-toxic nature, and eco-friendliness. At industrial application, there is a need for more advanced properties of an adsorbent such as fast adsorption kinetics, high capacity, and temperature stability. Polymer materials could be used as candidates to fulfill such industrial requirements. An inorganic hybrid polymer consisting of porous polymer beads loaded with monoclinic hydrous zirconium oxide, drew attention because it can remove oxoanions of Se(IV), Se(VI), As(III), As(V), and methyl derivatives of As(V) by electrostatic effects [12]. Silica-based zwitterionic hybrid polymers as adsorbents have been synthesized via Sol-Gel method [13]. For example, ring-opening polymerization of pyromellitic acid dianhydride (PMDA) and phenylaminomethyl trimethoxysilane followed by aqueous treatment and quaternization of the amine groups afforded zwitterionic hybrid polymers. Ionic groups of cationic quaternary amines and anionic carboxylic groups in zwitterionic polymers are involved in electrostatic interactions with heavy metals.

The production of total dyes exceeds the 700,000 tons per year [14]; the discharge of ≈2% of the total production in wastewater poses a serious environmental challenge owing to their high toxicity and carcinogenic and mutagenic characteristics [15]. Solid adsorbents, having advantages of low cost and simple operation without causing secondary pollution, are widely used to remove dyes from wastewater [16,17]. However, adsorbents like activated carbon, silica, zeolite, and chitosan, etc., have relatively low adsorption capacity owing to their weak affinity to HMI and dyes [18-21]. Graphene oxide (GO), as well as its decorated derivatives, have received considerable attention for environmental applications because of their enormous surface area [18, 22-24]. However, GO has its inherent problem of aggregation or agglomeration in aqueous

solution owing to the strong π–π interactions between graphitic layers; as a result, a low effective surface area put a limitation for wider application as adsorption materials [18, 25].

In the wastewater treatment, co-existence of heavy metal and ionic dyes constitutes the most dangerous source of environmental pollution. Several adsorbents such as magnetic graphene oxide, chitosan grafted with carboxylic groups, etc. have been synthesized and used for simultaneous removal of metal ion and ionic dyes [26,27]. The adsorption has been shown to be influenced by a variety of interactions such as electrostatic forces, hydrogen bonding, chelation, etc. There is a tremendous scope to develop new materials with high affinity to both HMI and dyes. Aminomethylphosphonate ($-NH^{+}CH_2PO_3H^{-}$) as a chelating ligand, has etched a place of distinction in the removal of heavy metal ions [28-30]. Having the pH-responsive zwitterionic motifs, the ligand may be tuned to trap metal cations, toxic anions (like AsO_4^{-}) as well as organic dyes of both algebraic signs. The affinity towards dyes may as well be augmented by the presence of hydrophobic aromatics capable of π-π interactions thereby leading to their association and entrapment. The goal of the work is to synthesize a novel functionalized resin with hydrophilic motifs of aminomethylphosphonate and hydrophobic pendants of 4-(6-hexyloxy)biphenyl as a sorbent for the removal of Cr(III) as a model case as well as several organic dyes from aqueous solutions (Scheme 1).

2. Experimental

2.1 Chemicals and Materials

Stock solutions of analytical grade Cr(III) nitrate (1000 mg/L), HNO_3, HCl, and NaOH were purchased from Sigma-Aldrich, USA. The standard stock solution was diluted to the predetermined concentrations for the adsorption tests. 2,2′-Azoisobutyronitrile (AIBN) (from

Fluka AG) was crystallized from a chloroform-ethanol mixture. Dimethylsulfoxide (DMSO) was purified by drying (CaH_2) and distilling at 64-65°C (4 mmHg). Monomer **1** (≈100% purity, was prepared by a modified procedure which avoided silica gel chromatography) [31]. Cross-linker **3** [32] was synthesized using a literature procedure. 4-(6-Bromohexyloxy)biphenyl: Ph-$PhO(CH_2)_6Br$ were prepared as described [33]. Chromium standard solution (1000 ppm) was used to prepare the diluted solutions of the required concentrations. Millipore water (18.2 MΩ·cm) was used for the adsorption study.

2.2. Characterization Techniques and procedures

Perkin Elmer Elemental Analyzer Series 11 Model 2400 (Waltham, Massachusetts, USA) was used for elemental analysis, while IR analyses were performed on a Thermo scientific FTIR spectrometer (Nicolet 6700, Thermo Electron Corporation, Madison, WI, USA) with deuterated triglycine sulfate detector. The background correction of the spectra was performed by 16 scans with a resolution of 2 cm^{-1}. NMR spectra were collected in a JEOL LA 500 MHz spectrometers using $CDCl_3$ with tetramethylsilane (TMS) as internal standard (^1H signal at δ 0 ppm), while in D_2O, residual proton HOD signal at δ4.65 ppm and dioxane ^{13}C signal at 67.4 ppm were taken as internal and external standards, respectively. ^{31}P was referenced with 85% H_3PO_4 in DMSO. The resin's morphology was examined by Scanning electron microscope (SEM). Energy-dispersive X-ray spectroscopy (EDX) fitted with an X-Max detector was used to get the elemental spectra of the resin.

The thermal stability of the resin was evaluated by Thermogravimetric analysis (TGA) with an SDT Q600 thermal analyzer from TA instruments, USA. The temperature was raised at a rate of 10°C/min over a temperature range 20–800°C using Platinum/Platinum–Rhodium (Type R)

thermocouples under air flowing at a rate of 100 mL/min. A thermogravimetric and differential scanning calorimetry (TGA-DSC) thermal analysis was performed on the sample to understand the thermal stability of the adsorbent.

The BET surface area, pore size, and volumes of the samples were measured on micromeritics Tristar surface area and porosimetry analyzer (Micromeritics, USA) using liquid N_2 adsorption-desorption at -196 ^oC by the methods of Brunauer-Emmett-Teller (BET) and Barrett-Joyner-Halenda (BJH). Prior to measurement, the samples were degassed at 150 ^oC for 3 h to remove the presence of impurities or moisture. The contribution of micropore and mesopores was computed from the *t*-plot method according to Lippens and de Boer. Atomic Absorption Spectroscopy (Thermo Scientific iCE 3000) was employed to monitor the concentration of Cr(III). The concentration of the tested dyes was monitored in a UV-vis spectrophotometer using optical quartz cuvettes. Inductively Coupled Plasma – Mass Spectrometer (ICP-MS) technique was employed to analyze the real wastewater samples.

2.3 Synthesis of monomers 2

A solution of 4-(6-bromohexyloxy)biphenyl Ph-PhO$(CH_2)_6$Br (3.33 g, 10.0 mmol) and diallylamine (4.9 g, 50 mmol) in toluene (5 mL) was heated under N_2 at 100 °C for 24 h. The reaction mixture, taken up in ether (50 mL), was washed with 5% NaOH solution (20 mL). The organic extract was dried (Na_2SO_4), concentrated and purified by chromatography over silica gel using ether/hexane mixture as eluent to obtain 4-(6-hexyloxybiphenyl)diallylamine (3.0 g, 86%) which on treatment with dry HCl in ether afforded monomer **2** as a white solid in quantitative yield. M.p. 108-110 °C; (Found: C, 74.4; H, 8.4; N, 3.6%. $C_{24}H_{32}ClNO$ requires C, 74.68; H, 8.36; N, 3.63). $\nu_{max.}$ (KBr) 3478, 3402, 3327, 3224, 3084, 3029, 2946, 2867, 1653, 1623, 1606,

1518, 1488, 1392, 1289, 1270, 1244, 1194, 1176, 1116, 1043, 1021, 997, 944, 848, 821, 772, 720, and 701 cm^{-1}; δ_H ($CDCl_3$) 1.42 (2H, quint, *J* 7.3 Hz), 1.53 (2H, quint, *J* 7.3 Hz), 1.80 (2H, quint, *J* 6.7 Hz), 1.89 (2H, m), 2.96 (2H, m), 3.63 (4H, m), 3.98 (2H, t, *J* 6.4 Hz), 5.52 (4H, m), 6.14 (2H, m), 6.95 (2H, d, *J* 8.6 Hz), 7.29 (1H, t, *J* 8.3 Hz), 7.41 (2H, t, *J* 7.6 Hz), 7.52 (2H, d, *J* 8.8 Hz), 7.54 (2H, d, *J* 8.3 Hz), 12.48 (1H, s).

2.4. Resin synthesis

*2.4.1. Quadripolymerization of monomers **1**, **2**, cross-linker **3** and SO_2 to hydrophobic cross-linked polyzwitterionic acid (HCPZA) **4***

Sulfur dioxide was absorbed (1.96 g, 30.6 mmol) onto a solution of **1** (4.56 g, 20 mmol), **2** (2.00 g, 5.0 mmol), and **3** (0.890 g, 2.78 mmol) in DMSO (16 g) in a RB flask (50 cm^3). Initiator AIBN (250 mg) was added under N_2, and the mixture was then stirred in the closed flask at 65 ºC. Within 1 h, the mixture became an immovable transparent gel, and the polymerization was continued at 65 ºC for 24 h. The flask was cooled and opened every 8 h to release N_2 produced during the decomposition of the initiator. Finally, the white resin was washed with a liberal excess of water and acetone. Resin HCPZA **4** was dried under vacuum at 65ºC for 6 h (7.8 g, 83%). The resin was found to have: C, 39.1; H, 6.3; N, 4.9; S, 11.2. HCPZA **4** containing **1** (72.0 mol%), **2** (18.0 mol%), **3** (10.0 mol%) and SO_2 (100 mol%) requires C, 39.63; H, 5.98; N, 5.12; S, 11.72%.

*2.4.2. Conversion of HCPZA **4** to hydrophobic cross-linked dianionic polyelectrolyte (HCDAPE) **5***

Resin **4** (0.50 g, 1.6 mmol) was treated with NaOH (0.18 g, 4.5 mmol) in water (5 mL); after 1 h at room temperature, a mixture of methanol (20 mL) containing NaOH (0.18 g, 4.5 mmol) was added to the gel. After filtering and washing with methanol, the resultant HCDAPE **5** was dried under vacuum for 6 h at 65 °C (0.51 g, 90%).

The resin was found to have: C, 37.2; H, 5.2; N, 4.5; S, 10.3. HCDAPE **5** containing repeating units derived from **7** (72.0 mol%), **6** (18.0 mol%), **8** (10.0 mol%) and SO_2 (100 mol%) requires C, 37.52; H, 5.09; N, 4.64; S, 10.63%. $\nu_{max.}$ (KBr) 3420 (v broad), 2093, 1657, 1520, 1486, 1418, 1299, 1123, 1066, 976, 845, 766, and 557 cm^{-1}.

2.5. Swelling coefficient

The swelling coefficient is the ratio of the wet volume of the resin to the dry volume. The swelling coefficient was evaluated as follows: resins were properly crushed and a 20- to 30-mesh fraction was used. To a certain volume of the dry resin in a burette, sufficient water was added to cover its level; the equilibrated volume of the wet sample was measured and compared with the volume of the dry resin.

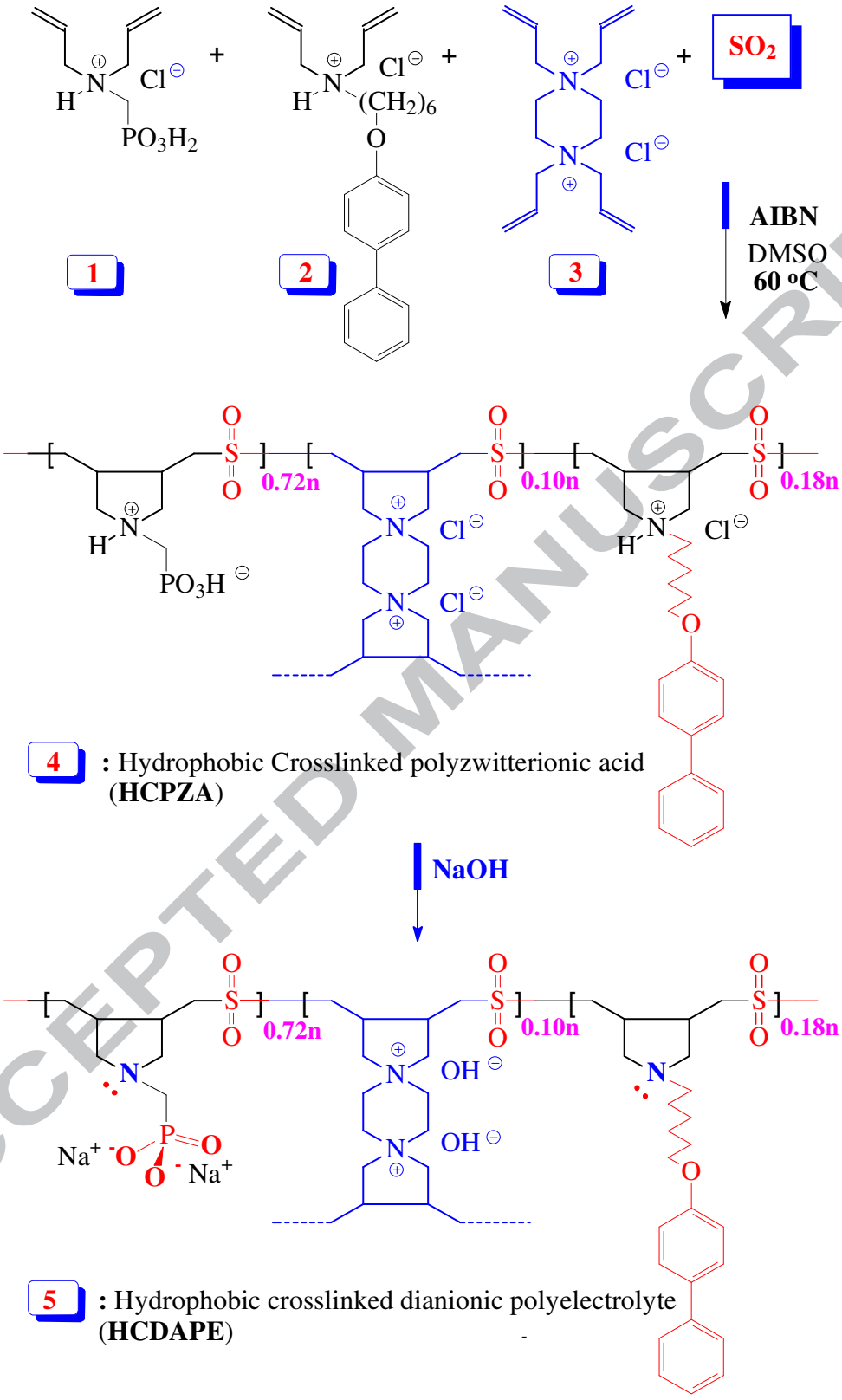

Scheme 1. Synthesis of a hydrophobic resin.

2.6. Batch Experiments

Adsorption efficiency was assessed by the batch experiments carried out as follows: 5, 10 and 20 mg of resin **4** was mixed in aqueous Cr(III) solution (40 mL) and stirred at various periods during 120 min at 298 K. The initial concentration of Cr(III) was 1.0 ppm. The Cr(III) solution was then filtered and analyzed by AAS to quantify the Cr(III) ion uptake. To gain thermodynamic and kinetic data, batch experiments were performed at temperatures of 298, 318 and 338 K.

The binary system experiments were performed using 30 mg of resin **4** in aqueous solution (20 mL) having 1 ppm concentration of each of Cr(III) and dyes. The resultant solutions were analyzed by ICP for Cr(III) ions, while UV-Vis spectrometer was used for the analysis of dye compounds: methyl orange, eriochrome black T, rhodamine B, methyl red and methylene blue.

The kinetic studies were performed under the optimized conditions of shaking speed (150 rpm) and pH (5). After the equilibrium, final methyl orange, Eriochrome black T, rhodamine B, methyl red and methylene blue concentrations were analyzed using UV–Vis spectrophotometer and the Cr(III) concentration was monitored by flame atomic spectroscopy.

2.7. Data Analysis

The percent removal of Cr(III) at the equilibrium was calculated by the equation:

$$\%\,Removal = \frac{C_\circ - C_e}{C_\circ} \times 100 \qquad (1)$$

Adsorption capacities were calculated using the equations:

$$q_e = (C_o - C_e) \times \frac{V}{m} \qquad (2)$$

and

$$q_t = (C_o - C_t) \times \frac{V}{m} \quad (3)$$

In equation (2), the adsorption capacity q_e (mg g^{-1}) at equilibrium is the amount of Cr(III) adsorbed per gram of the resin. Meanwhile, in equation (3), the adsorption capacity q_t (mg g^{-1}) is the adsorbed Cr(III) (mg) per gram of **4** at time *t*. C_o, C_e and C_t are the initial concentration (mg L^{-1}) of Cr(III) and its concentrations at the equilibrium and at time *t,* respectively. *V* (L) and *m* (g) stand for the solution volume and the mass of the resin, respectively.

2.8. Adsorption/Desorption experiment

After stirring resin **4** (20 mg) in 1.0 ppm Cr(III) solution (40 mL) at pH 5 for 24 h and then centrifuging, the q_e value was determined by AAS to quantify the Cr(III) ion left in the supernatant liquid. For the desorption process, the metal ions- loaded resin in the centrifuge tube was washed with the pH 5 buffer solution, then treated with 0.1 M HNO_3 (20 mL) at room temperature for 6 h. The concentrations of the desorbed metal ions were determined and used to calculate the efficiency of desorption process. The resin left in the centrifuge tube was washed with deionized water; as described above, the adsorption/desorption procedure was repeated three times. It is worth mentioning that the procedure ensured the use of a fixed amount of the same resin three times. Centrifugation ensured no loss of the resin as it may happen in the usual filtration procedure.

Similar adsorption/desorption experiments were carried out for a Cr(III)-Eriochrome Black Tea binary system. As described before, the adsorption experiment for binary systems were performed using 30 mg of resin **4** (20 mg) in aqueous solution (40 mL) having 1 ppm concentration of each of Cr(III) and Eriochrome Black Tea at pH 5. After centrifuging, the supernatant solutions were analyzed by ICP for Cr (III) ions, while UV-Vis spectrometer was

used for the analysis of the dye. The regeneration tests were conducted by washing the loaded resin with acetone to remove Eriochrome Black Tea and, as before, by treating with 0.1 M HNO_3 for the removal of Cr(III).

3. Results and discussion

3.1. Synthesis and characterization

Cyclopolymerization protocol [34,35] was employed in the AIBN-initiated quadripolymerization of hydrophilic monomer **1**, hydrophobic monomer **2** and cross-linker **3**, along with SO_2 as the fourth alternating monomer to obtain hydrophobic cross-linked polyzwitterionic acid (HCPZA) **4** in 83% yield (Scheme 1). During the work up, HCl is eliminated to give the zwitterionic aminophosphonate motifs. The composition of the repeating units in the resin matched with the feed ratio of 0.72: 0.18 : 0.10 : 1.0 for monomers **1/2/3/**SO_2 as supported by elemental analysis: This is expected for such a high conversion of the monomers to the resin.

HCPZA **4** upon treatment with NaOH was converted to HCDAPE **5**. Zwitterionic resin **4** and its anionic form **5** were found to have swelling coefficients of 1.8 and 6.3, respectively. The zwitterionic form of a compact coil in **4** is expected to have a lower affinity for adsorption of water, while the anionic form **5** has more expanded conformations owing to the repulsion among negative charges and thus has a greater affinity for solvation. The presence of the hydrophobic units and chelating aminophosphonate ligands in the resin would serve dual purposes: with a single treatment, the removal of organic pollutants and toxic metal ions is anticipated.

The FTIR spectra of the resin **4** and Cr(III)-loaded resin are depicted in Fig. 1. The asymmetric and symmetric bands of SO_2 appeared at ≈1310 cm^{-1} and ≈1124 cm^{-1}, respectively. The bands at 560 – 600 cm^{-1} and 1000–1100 cm^{-1} regions can be assigned to phosphonate groups [36]. Adsorbed water band is seen at around 3400 cm^{-1}, while the band at 1620 cm^{-1} is assigned to the bending vibration of H_2O. The peak at 1477 cm^{-1} is attributed to the C-N stretching. The absorption band at 1075 and 1190 cm^{-1} were assigned to the ν_s (PO_2) and and ν_{as} (PO_2) of PO_3H^- [31].

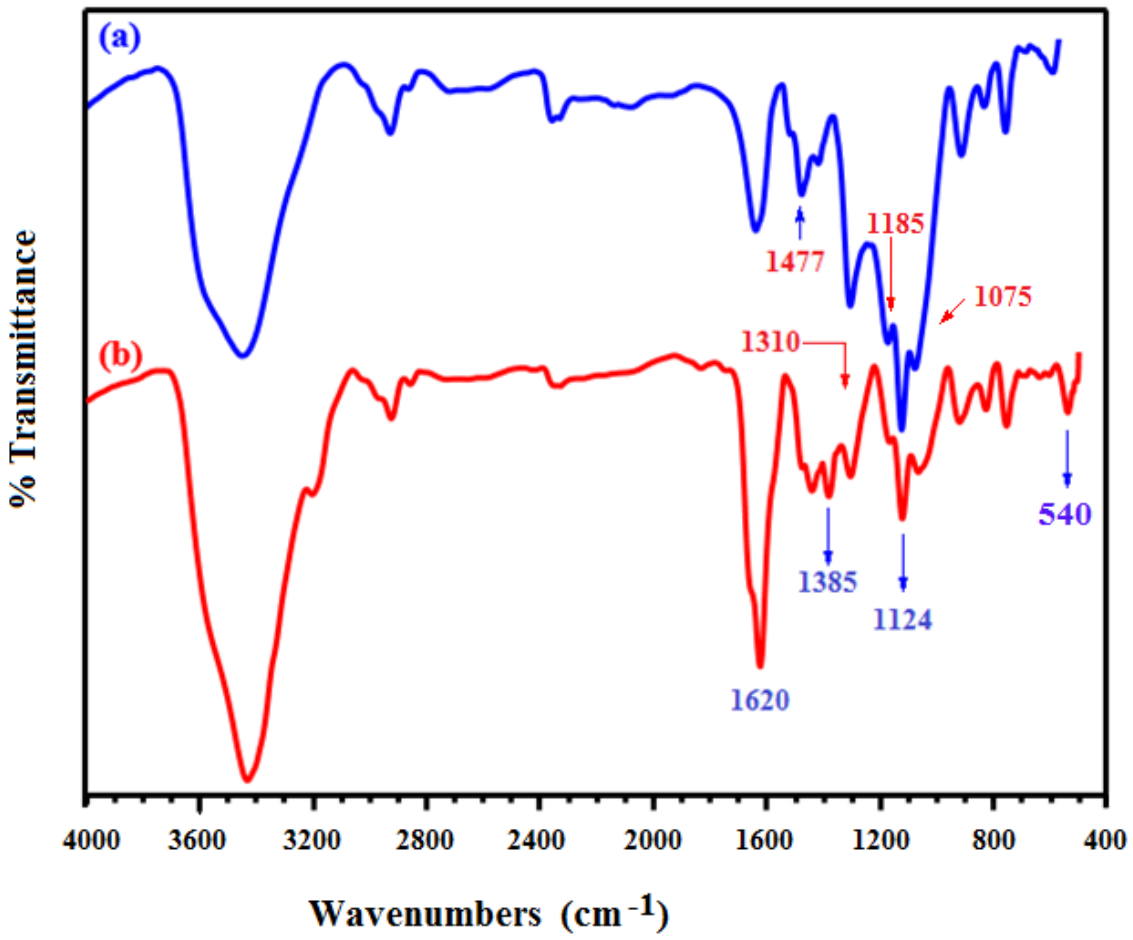

Fig. 1. IR Spectra of (a) resin **4** and (b) Cr(III)-loaded resin **4.**

[The preparation of loaded Sample; Resin: 50 mg; initial [Cr(III)]:100 ppm, volume of adsorption medium: 20 mL, Initial pH: 5.0, stirring time: 300 rpm, overnight, Temperature: 298 K].

The N_2 adsorption-desorption isotherm displayed by the polymer is given in Fig. 2. It showed a resemblance of Type I isotherm. The presence of hysteresis loop at high relative pressure signified the presence of mesopores, while the uptake of nitrogen at low relative pressure confirmed the presence of micropores in the sample. The textural parameters obtained quantitatively were summarized in Table 1 [22]. The resin's surface area of 56 m^2/g is indeed relatively high for an ionic resin [28]. The higher surface area may be attributed to the presence of long hydrophobic tail in **4** requiring larger space in the resin matrix.

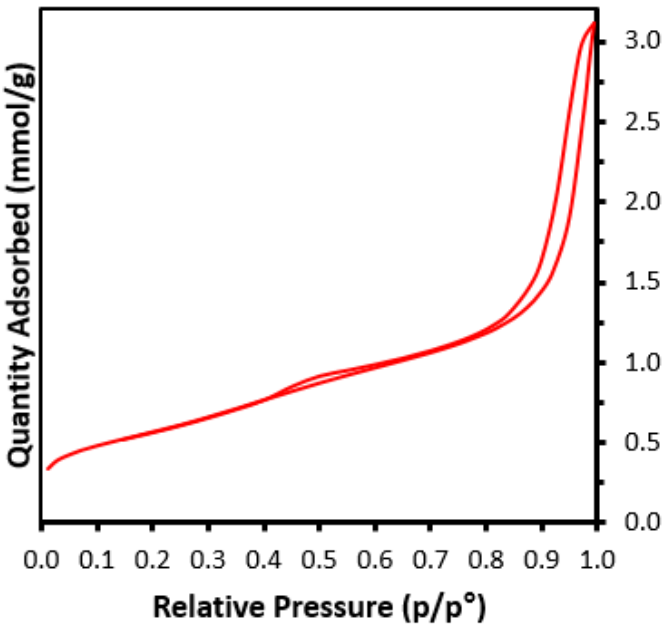

Fig. 2. BET adsorption-desorption curves of the polymer sample.

Table 1.

Properties of resin **4** obtained from BET surface

area analysis.

Textural Parameters	Values
BET surface area (S_{BET})	56 m^2g^{-1}
Micropore surface area (S_{micro})	19 m^2g^{-1}
Mesopore surface area (S_{meso})	23 m^2g^{-1}
Total pore volume (V_t),	0.67 cm^3g^{-1}
Micropore volume (V_{micro})	0.08 cm^3g^{-1}
Average pore diameter (APD)	8.3 nm

The TGA curve of the prepared resin, depicted in Fig. 3, revealed two distinct weight loss stages. The first gradual loss of around 5% up to 225 °C can be assigned to the removal of the trapped moisture and HCl from the material. The second steep loss of ≈ 33% in the range 225-375 °C is assigned to the loss of phosphonate pendants and SO_2 owing to polymer degradation. The loss thereafter could be attributed to the combustion of functional groups releasing NOx, CO_2, and H_2O gasses [37]. As seen from the Figure, the resin remained stable even at 250 °C.

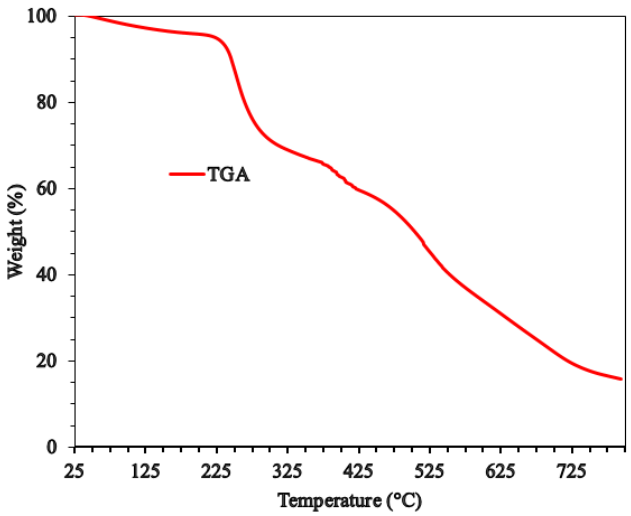

Fig. 3. TGA curve of resin **4**.

3.2. Evaluation of Adsorption efficiency

3.2.1. pH-responsiveness

The dependency of the Cr(III) removal on the pH was studied in the pH range 3-7 using dosages of 5, 10 and 20 mg of the resin in 40 mL aqueous mixture, and the results are depicted in Fig. 4. Solutions of pH > 7 were not examined to avoid the competition between the adsorption and precipitation of the Cr in form of $Cr(OH)_3$. Note that the pH can affect the nature of the chelating motifs in the resin (Scheme 1). Adsorption of Cr(III) ions increased with the increase in pH in the range 3 - 7 and the optimum pH value was found to be in the range 5 - 7.

The trend depicted in Fig. 4 is explained by considering the surface charge of the resin. The active sites on the resin, play a key role in the removal of Cr(III). At pH > 6, chromium is precipitated as chromium hydroxides [23, 38], while the dominant species in solutions having pH in the range 1 – 6 are $CrOH^{2+}$, $Cr_3(OH)_4^{5+}$ and $Cr_2(OH)_2^{4+}$. The positively charged species are attracted to the negative sites (PO_3H^- and PO_3^{2-}) on the resin. In the solution of low pH of 3, the hydronium ions effectively compete with the chromium species for the adsorption sites on the resin, thereby decreasing its adsorption capacity.

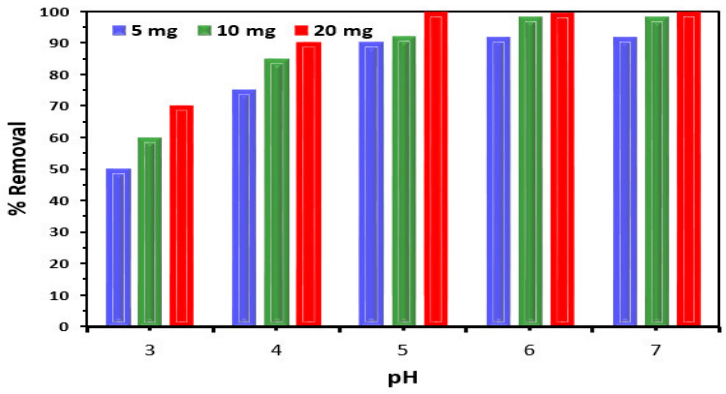

Figure 4. Effect of the pH of the solution on percent Cr(III) removal using various dosages of resin **4**.

[Experimental conditions; the amount of resin: ■ 5, ■ 10 and ■ 20 mg, the volume of the medium: 40 mL, temperature: 298 K , initial concentration of Cr(III): 1.0 ppm].

3.2.2. Contact Time

The batch experiments with a resin dosage of 5, 10, and 20 mg in solution (40 mL) having initial concentration of Cr(III) were carried out at 25 ºC to evaluate the dependence of the adsorption capacity on the contact time. Initially, the rate of adsorption of Cr(III) was fast with steep slopes, while it attained equilibrium adsorption value within 20 min at a resin dosage of 20 mg (Fig.5).

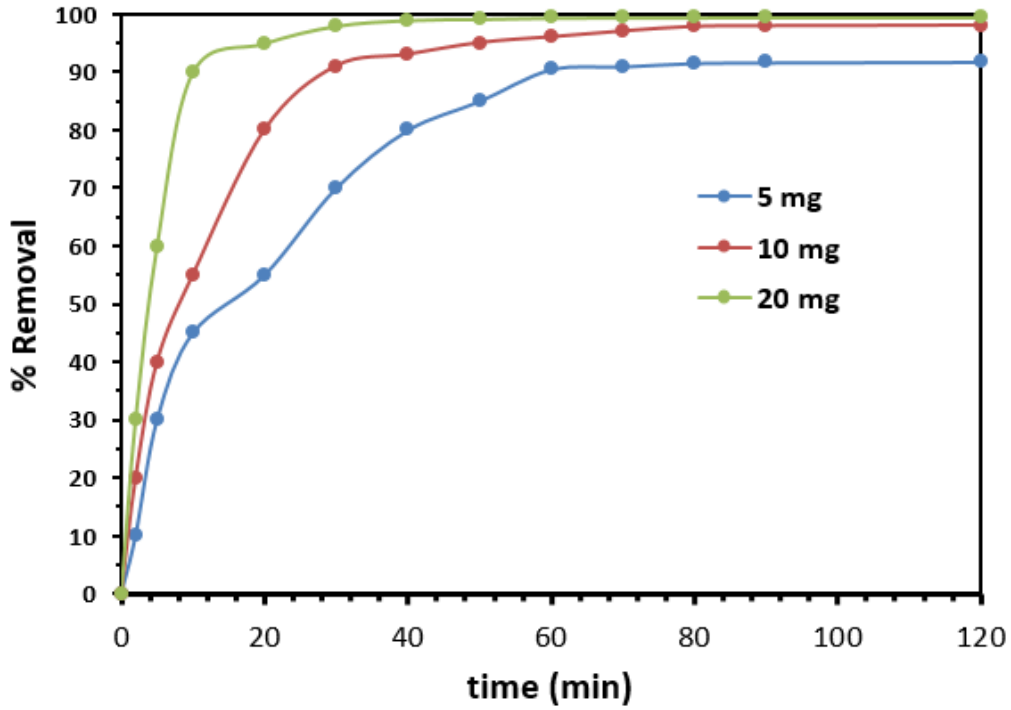

Fig. 5. Dependency of percent removal of Cr(III) versus contact time with solution containing various dosages of the resin.
[Experimental conditions; amount of resin: ● 5, ●10 and ● 20 mg, volume of medium: 40 mL, temperature: 298 K , initial concentration of Cr(III): 1.0 ppm].

3.2.3. Kinetics

Lagergren's first and pseudo-second-order kinetic models were applied to examine the adsorption mechanisms. For the first-order kinetics, linear equation (4) was used [39]:

$$\ln(q_e - q_t) = \ln q_e - k_1 t \quad (4)$$

where the amounts of Cr(III) (mg/g) adsorbed at t and at equilibrium are described by q_t and q_e respectively, while k_1 represents the rate constant. The ln (q_e - q_t) versus t plot yielded k_1 and q_e, values (Fig. 6a, Table 2). Disagreement between the experimental ($q_{e,\,exp}$) and calculated value ($q_{e,\,cal}$), and the poor correlation coefficients (R^2) ruled out the adsorption rate obeying the first-order kinetic model. The second-order adsorption rate was obtained using [40]:

$$\frac{dq_t}{dt} = k_2(q_e - q_t)^2 \quad (5)$$

where k_2 represents the rate constant, and q_e and q_t are the respective adsorption capacities at equilibrium and at time t.

The pseudo-second-order in the linear form is written as:

$$\frac{t}{q_t} = \frac{1}{k_2 q_e^2} + \frac{t}{q_e} \quad (6)$$

where k_2 is obtained from t/q_t versus t plot (Fig. 6b). The high correlation coefficient values, and agreement between $q_{e,\,cal}$ and the $q_{e,\,exp}$ supported the adsorption process as following the pseudo-second order kinetics model involving predominant chemical interaction between Cr(III) and the chelating ligands (Table 2).

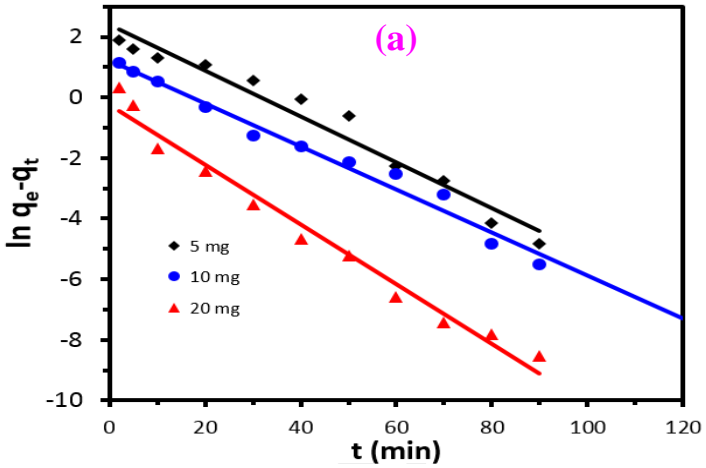

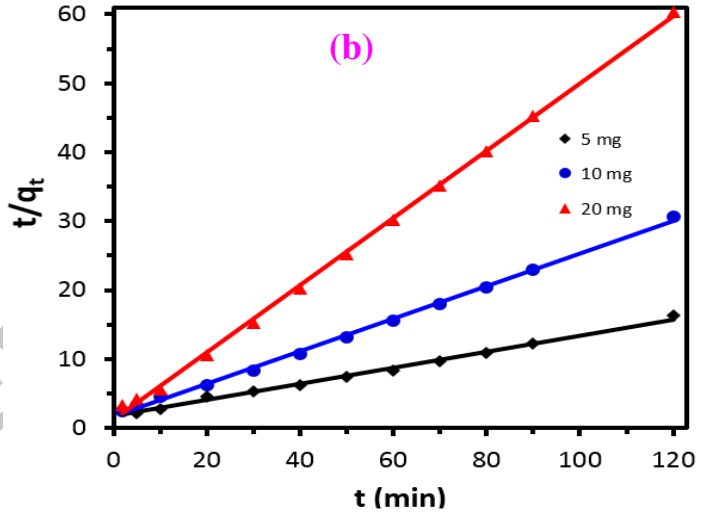

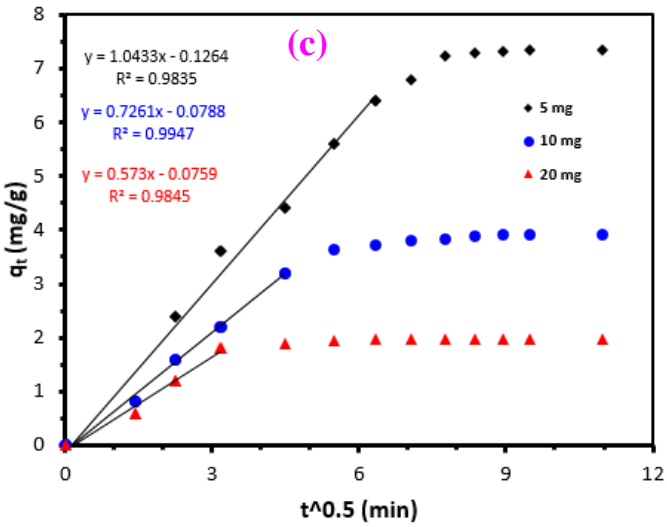

Fig. 6. (**a**) Lagergren's psudo-first order; (**b**) Pseudo-second order and (**c**) Interparticle diffusion model at 298 K.

[Experimental conditions; amount of resin: ♦ 5, ●10 and ▲ 20 mg, volume of medium: 40 mL, temperature: 298 K, initial concentration of Cr(III): 1.0 ppm].

Table 2

Kinetic parameters for Cr(III) [a] adsorption on the resin at 298 K.

Resin (mg)	q_e, exp (mg/g)	Lagergren's Pseudo first-order			Pseudo second-order			Intraparticle diffusion		
		k_1 (min^{-1})	q_e, cal (mg/g)	R^2	k_2 [b]	q_e, cal (mg/g)	R^2	k_{id} [c]	C (mg/g)	R^2
5	7.34	0.0757	11.0	0.9646	0.00801	8.55	0.9983	0.881	6.87	0.9975
10	3.92	0.0987	3.41	0.9778	0.0294	4.76	0.9988	0.650	5.89	0.9798
20	1.99	0.0711	3.32	0.9796	0.146	2.51	0.9998	0.542	2.91	0.9896

[a] Intitial Cr(III) concentration: 1.0 ppm and solution volume (40 mL).

[b] (g/mg•min).

[c] (mg/g•min).

The adsorption results were fitted using Weber's intraparticle diffusion model [41-46]:

$$q_t = k_{id} t^{1/2} + C \quad (7)$$

where a k_{id} (mg/g• $min^{1/2}$) is the constant of intraparticle diffusion rate, C is the intercept (mg/g). The experimental data expressed that initially, the plots of q_t versus $t^{1/2}$ are linear with very good correlation coefficients and passing through the origin (C = ≈ 0), thereby implicating intraparticle diffusion as the rate-limiting step [47,48]. It can be discerned from Fig. 6c that the initial linear portion represents the intraparticle diffusion while the plateau represents the equilibrium.

3.2.4. Adsorption Isotherms

Isotherms models provide fundamental physiochemical data to assess adsorption capacity. Langmuir isotherm, the ideal localized monolayer model, is based on the concept of a homogeneous surface phase. It is used to describe the nature of the process either a physical or chemical, using the equation [42]:

$$\frac{C_e}{q_e} = \frac{1}{k_L q_m} + \frac{C_e}{q_m} \quad (8)$$

where k_L (L/mg), q_m (mg/g), C_e (mg/L), and q_e (mg/g) represent the affinity of adsorption sites; theoretical monolayer adsorption capacity, the equilibrium concentration of Cr(III) and its amount adsorbed per gram resin, respectively.

The plot of C_e/q_e versus C_e is depicted in Fig. 7a, where the slope and intercept gave the k_L and Langmuir constant q_m, respectively (Table 3). The separation factor represented by the dimensionless equilibrium parameter R_L is introduced in eq (9) [43]:

$$R_L = \frac{1}{1 + K_L C_o} \quad (9)$$

where C_o represents the initial solute concentration. The adsorption process becomes unfavourable for R_L>1, linear for R_L = 1, favourable for 0 < R_L< 1, and irreversible when R_L = 0. As shown in Table 3, the favorability of the adsorption is confirmed by the R_L value of 0.57. For the sake of comparison, the maximum adsorption capacity (q_m) of the current resin and some other sorbents reported for the removal of Cr(III) are tabulated in Table 4; the current resin was found to be more effective than the other sorbents.

Table 3

Langmuir, Freundlich and Temkin isotherm parameters for the adsorption of Cr(III) on resin **4**.

Langmuir				Freundlich				Temkin		
q_m (mg/g)	k_L (L/mg)	R_L	R^2	1/n	n	k_f (mg/g)	R^2	K_T (L/g)	b_T (kJ/mol)	R^2
16	40	0.57	0.9899	0.4756	2.10	24.5	0.9984	1.006	1.29	0.9799

Table 4

Comparison between the efficiency of the resin with literature reported adsorbents.

Adsorbent	Initial Conc. (mg/L)	pH	Cr(III) removal efficiency	Loading Capacity (mg/g)	Ref.
Lewatit S: Sulfonic acid group with cross linked polystyrene matrix	52	3.5	99	20	[49]
Amberlite Sulfonic acid group	10	5	87	2.2	[50]
Styrene-DVB	20	5.5	68	2.5	[51]
Coconut shell carbon	50	6	87	20	[52]
Sulfonated styrene/acrylonitrile Sulfonatedpolymethylmethacrylate	30	6	90	7.2 9.0	[53]
Polymer	1.0	5.5	99	16	(Current work)

The Freundlich model describes the adsorption characteristics on heterogeneous surfaces where the adsorbed molecules interact among them [44] and is expressed as:

$$q_e = K_f C_e^{\frac{1}{n}} \quad (10)$$

where Freundlich isotherm constant K_F (mg/g) and $1/n$ indicates the adsorption capacity and its intensity, respectively. C_e and q_e describe the concentration (mg/L) of the adsorbate and its amount adsorbed per gram of the adsorbent (mg/g) at equilibrium. The model in linear for is:

$$\ln q_e = \ln K_f + \frac{1}{n} \ln C_e \quad (11)$$

where K_F and n values as calculated from the ln q_e versus ln C_e plot (Fig. 7b) are included in Table 3. The n value is used to describe the nature of the adsorption process: 1/n <1 and > 1

imply a normal and a cooperative adsorption, respectively. The 1/n value of ≈ 0.5 in the current work indicates a favorable adsorption process.

The Temkin model considers the interactions between the adsorbent and adsorbate, and it assumes a linear decrease in the adsorption energy as given by [31]:

$$q_e = \frac{RT}{b_T} \ln K_T + \frac{RT}{b_T} \ln C_e \qquad (12)$$

where Temkin isotherm constant b_T describes the heat of sorption (J mol^{-1}), while Temkin isotherm equilibrium binding constant k_T reflects the maximum binding energy (L/g). R and T represent the gas constant (8.314×10^{-3} kJ/mol.K) and temperature (K), respectively. The q_e versus ln C_e plot gave the isotherm constants (Fig. 7c).

As shown in Table 3, the square of correlation coefficients (R^2) for the Langmuir and Freundlich are found to be excellent and very close, while for the Temkin, the data fit the isotherm reasonably well. The adsorption of Cr(III) by the resin could thus be considered a monolayer adsorption on a heterogeneous surface.

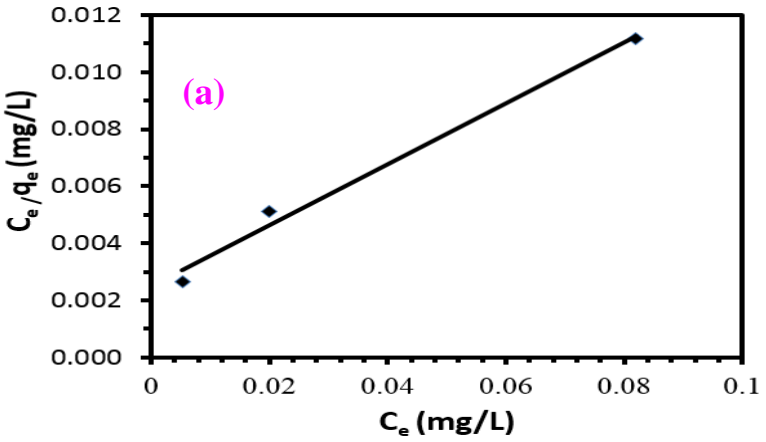

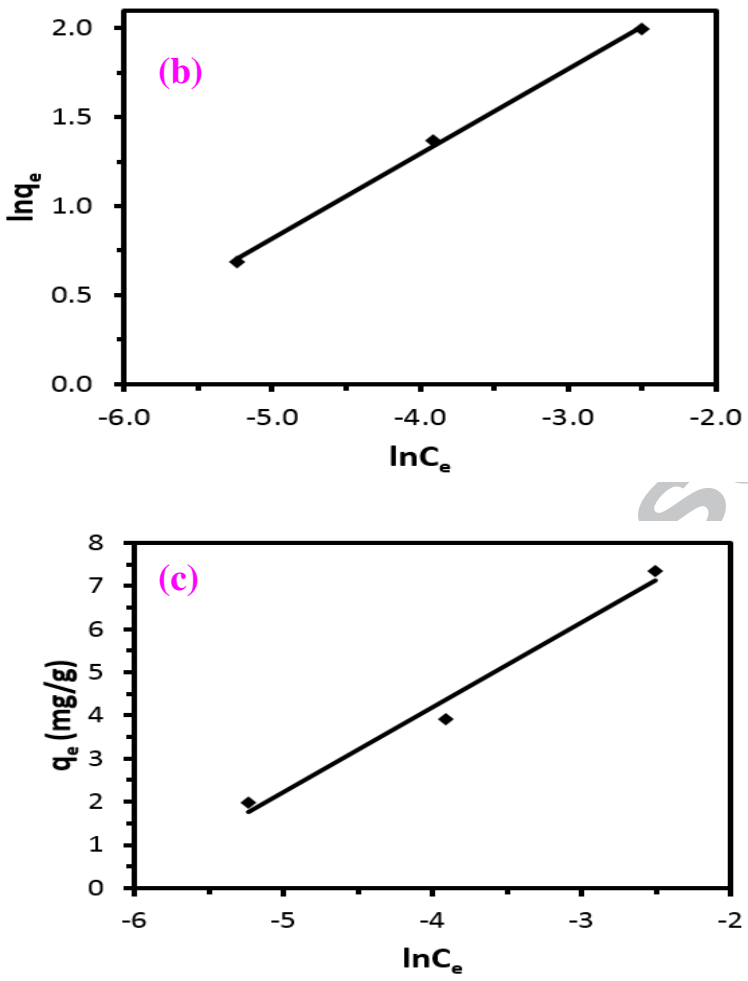

Fig. 7. (**a**) Langmuir, (**b**) Freundlich and (**c**) Temkin adsorption isotherms for the removal of Cr(III) using the adsorbent. [Experimental conditions; amount of resin: 5.0, 10, 20 mg, volume of medium: 40 mL, temperature: 298 K, initial concentration of Cr(III): 1.0 ppm), initial pH: 5.0].

3.2.5. Energy of activation and Thermodynamics

Using Arrhenius equation [Eq. (13)] and the related plot (Fig. 8a), the activation energy E_a for the adsorption of Cr(III) was determined to be 42.8 kJ/mol which is at the higher end of the range 5 – 40 kJ/mol, considered as the energy requirement for a physisorption process. The adsorption may not be simply an ion exchange process, in addition, it may involve chemical exchange involving chelation.

$$\log k_2 = -\frac{E_a}{2.303RT} + \text{constant} \quad (13)$$

The thermodynamic parameters ΔG^o, ΔH^o and ΔS^o are used to describe the adsorption process. The data were collected using adsorption study at 298, 318 and 338 K with a resin dosage of 5 mg of resin in 1.0 ppm Cr(III) (40 mL). A plot of $\ln K_c$ versus $1/T$ (Fig. 8b) using Van't Hoff eq (13) in the linear form gave the ΔH^o and ΔS^o values which were used to compute the ΔG^o using eq (14):

$$\ln K_c = \frac{\Delta S^0}{R} - \frac{\Delta H^0}{RT} \quad (14)$$

$$\Delta G^0 = \Delta H^0 - T\Delta S^0 \quad (15)$$

The standard thermodynamic equilibrium constant K_c is equated to q_e/C_e (L/mg) [45, 46]. The decrease in ΔG^0 values (-3.4, -3.8, and -4.3 kJ/mol) with the increase in temperature and their negative sign reveals the adsorption as a favorable process. The positive ΔH^o value of 26 kJ/mol implies endothermic adsorption. The ΔS^o positive value of 5.9 J/mol.K indicates the affinity of the resin towards Cr(III) with an increase in randomness at the solid-solution interface.

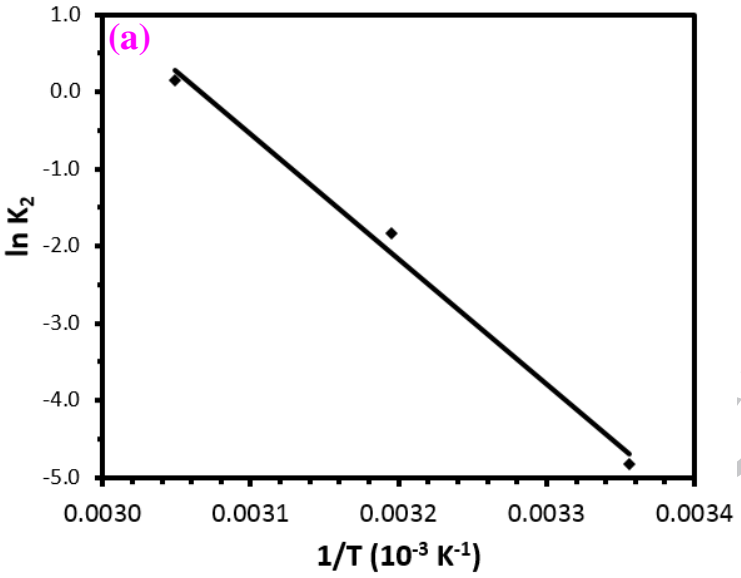

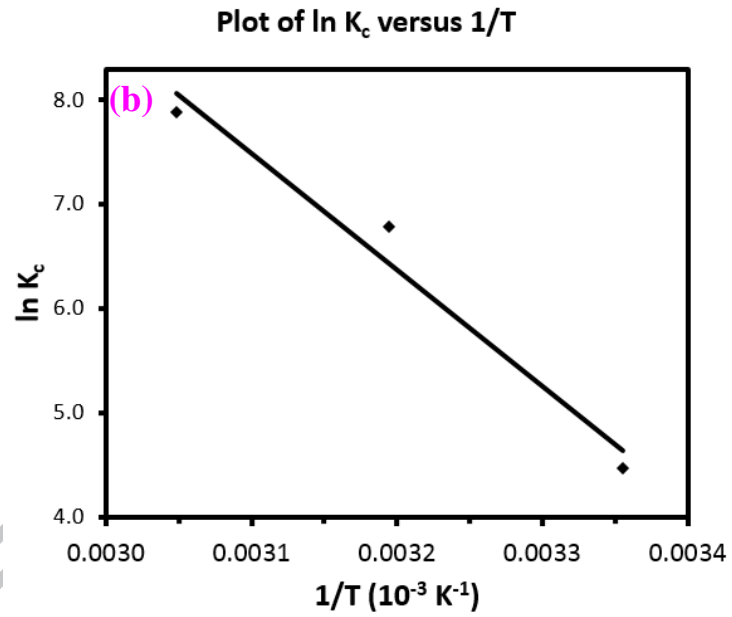

Figure 8. (**a**) Arrhenius plot of ln k_2 versus 1/T for Cr(III) adsorption on the resin and (**b**) Plot of ln K_c versus 1/T.
[Experimental conditions; amount of resin: 5.0 mg, volume of medium: 40 mL, temperature: 298, 318, and 338 K, initial concentration of Cr(III): 1.0 ppm, initial pH: 5.0].

3.2.6. Characterization of the spent adsorbent

The resin's surface morphology and structure were evaluated using a scanning electron microscope (SEM), energy dispersive X-ray (EDX) analyses, elemental mapping and FTIR spectroscopy. The analysis of the adsorbate loaded resin was conducted using SEM and EDX. The resin (100 mg) was loaded with Cr(III) after stirring overnight in a 20 ppm Cr(III) solution (20 mL). As depicted in Fig. 9, one can notice the presence of the chromium in the EDX spectrum at 0.6 and 5.4 and 5.9 keV. It can be seen from EDX that Cr has a set of peaks on its electromagnetic emission spectrum, which accounted for 2.04 wt% of Cr being adsorbed on the resin.. The data thus confirm the possible binding of Cr(III) to the surface of the polymer. The low intensity of the Cr peaks in the EDX spectrum could be due to the use of low concentration of Cr(III).

The FTIR spectra of resin **4** and Cr(III)-loaded **4** are displayed in Fig. 1b. The shape of the absorption bands of the phosphonate groups at ≈1100 cm^{-1} (Fig. 1a) has been changed in Fig.1b because of bonding with Cr(III) ions, presumably because of chelation between the phosphonate groups and the chromium ions. The appearances of a new strong band 1385 cm^{-1} (Fig. 1b) can be assigned to the presence of nitrate ions since chromium nitrate was used in the experiments [46]. Interestingly, the presence of this band indicates the ability of the polymer to act as an anion exchanger [54] in addition to being cationic exchanger. This is due to the presence of charges of both algebraic signs in resin **4** at the pH of 5 (Scheme 1). It is not surprising since the resin has 10 mol% cross-linker having a permanent positive nitrogens of ≈20 mol% that can act as anion exchanger. Appearance of a peak at 540 cm^{-1} is attributed to Cr(III)-O bond formed through oxygen atoms of the phosphonic acid group [46]. The P-O peaks are perturbed in Cr(III)-loaded resin, thereby implying a complex formation between the metal ions and the phosphonate group [54, 55].

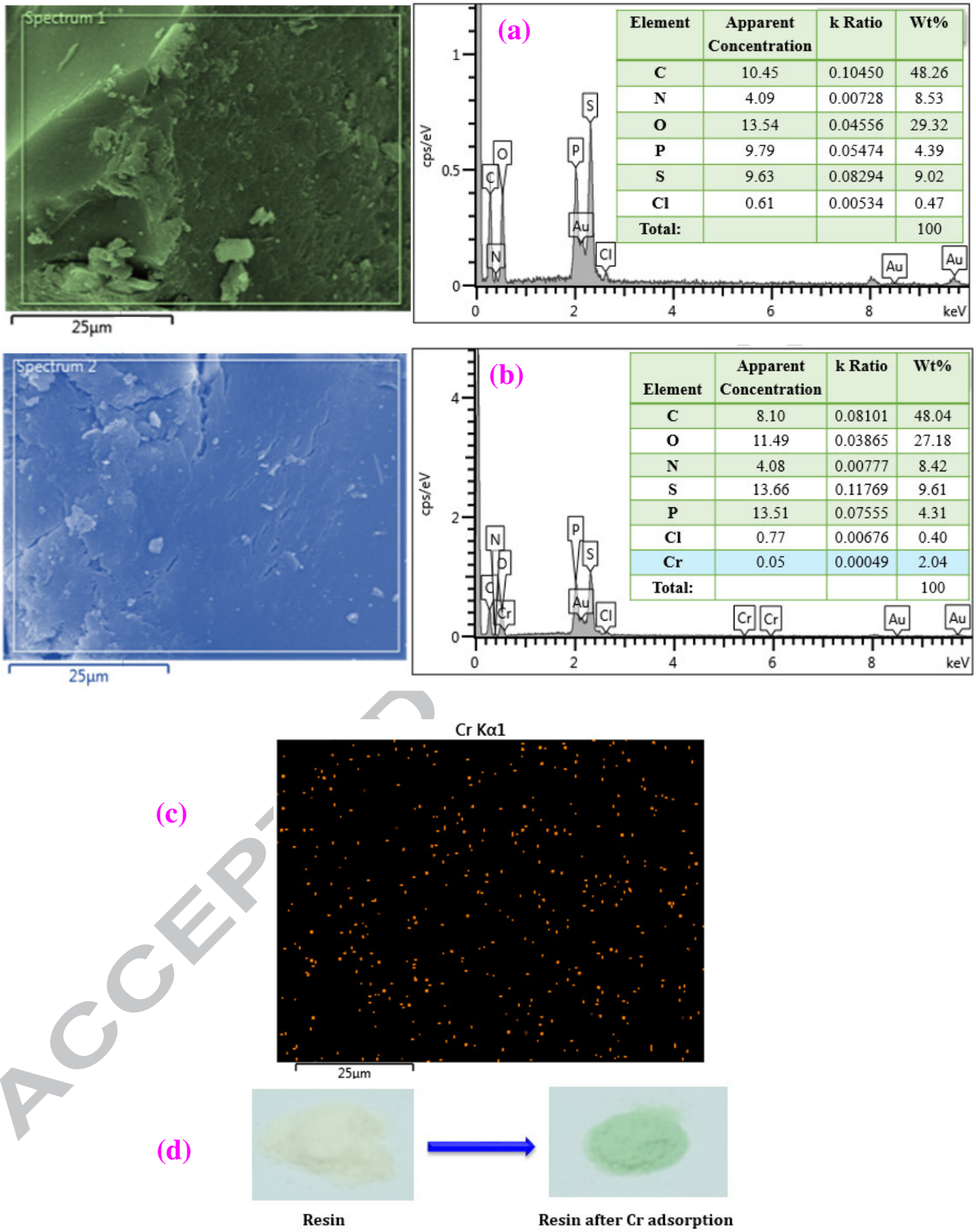

Fig. 9. SEM images and EDX spectra with a table of analysis of (**a**) the resin **4**, (**b**) Cr(III)-loaded resin and (**c**) Chromium elemental mapping of the Cr(III)-loaded resin; (**d**) photo showing the colour of the resin before and after the Cr adsorption.

3.3. Individual and simultaneous removal of dyes and metal ions from industrial wastewater

Since the resin was designed with hydrophobic branches that can attract the organic pollutants, it was also evaluated for the removal of various dyes (1 ppm each) in the presence of Cr (III). The resin showed remarkable efficiency in removing methyl orange, Eriochrome black T, rhodamine B, methyl red and methylene blue with efficiencies of ≈100, ≈100, 95, 92, and 90%, respectively, achieved in 30 min, while the results indicated ≈100% removal of Cr(III) as the Cr(III) level in the filtrate was found to be <MDL (i.e. 1 ppb). The changes in the color of the dye solutions before and after mixing with the resin are displayed in Fig. 10.

Thus, the results so far encouraged us to investigate the efficacy of the resin with a real sample. The industrial wastewater samples (pH 6.3) were used to study the effect of the matrix. The sample was spiked with 10000 ($\mu g\ L^{-1}$) Cr(III) and 1 ppm of methyl orange and Eriochrome black T, and then treated with the resin. The dye concentrations were analyzed using the UV-vis spectrophotometer. Table 5 presents the analysis of wastewater sample. The % removals are remarkable; the resin captured efficiently not only the metal ions but also arsenate ions, suggesting its efficiency as an anion exchanger. It is indeed pleasing to see the almost complete simultaneous removal of the dye as well as metal ions.

The regeneration of the used resin was successfully achieved by using 0.1 M HNO_3 at room temperature for 2 h. The polymer has demonstrated remarkable efficiency in removing toxic Cr(III) ions from waters even after 3 cycles with ±4% changes.

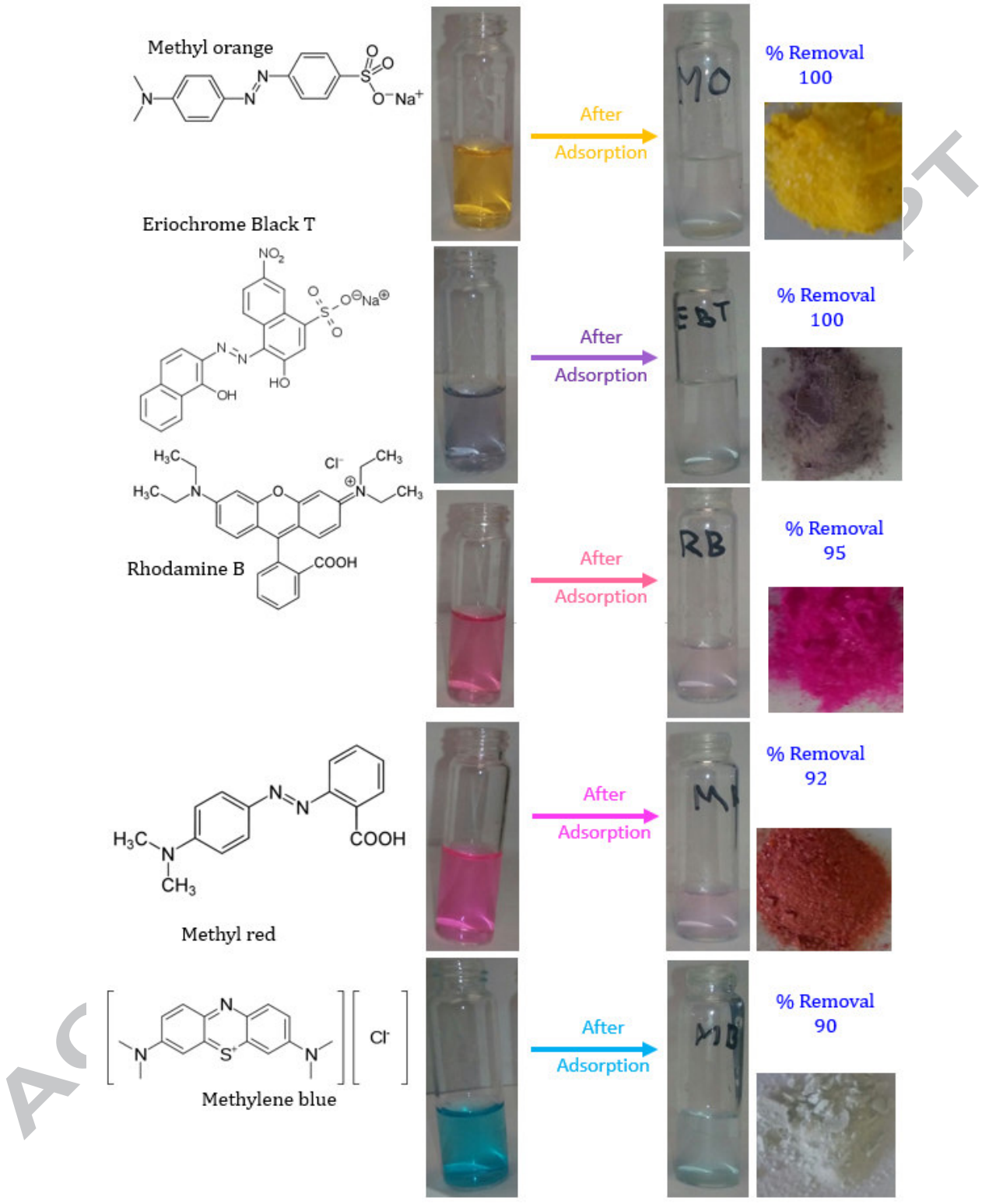

Fig. 10. Photos showing the change in the color of the dye solutions before and after mixing with the resin and the color of the solid resin after adsorption.

Table 5

Cr(III) and dye concentrations in wastewater sample before and after the treatment with the resin.

Metal	Original sample ($\mu g\ L^{-1}$)	Original sample *spiked* with 10000 ($\mu g\ L^{-1}$) Cr(III) and 1 ppm dyes; then treated with the polymer	Removal (%)
Cr	8.58	76.3	99
Pb	13.28	0.08	96
Cd	2.38	0.013	60
Cu	652.2	258	59
As	4.85	0.92	81
Mo	21.20	1.27	93
Ni	4.31	< MDL	≈100
Methyl orange	1 ppm	< MDL	≈100
Eriochrome black T	1 ppm	< MDL	≈100

MDL: the method detection limit

3.4. Reuse of the resin

For economic and environmental reason, recycling and reusability of the resin is an important aspect. As described in the experiment section, the adsorption/desorption experiments were repeated three times. The desorbed samples also demonstrated similar efficiency as the original sample. The resin shows good recovery with almost stable efficiency for the second and third adsorption/desorption cycles. The results of three (3) cycles of adsorption/desorption procedures are displayed in Fig. 11. The resin has demonstrated remarkable efficiency in removing toxic Cr(III) ions from waters even after 3 cycles with ± 4% changes. For binary systems, the efficiency remained stable within ± 3-4% for the removal of Cr(III) and Eriochrome Black T.

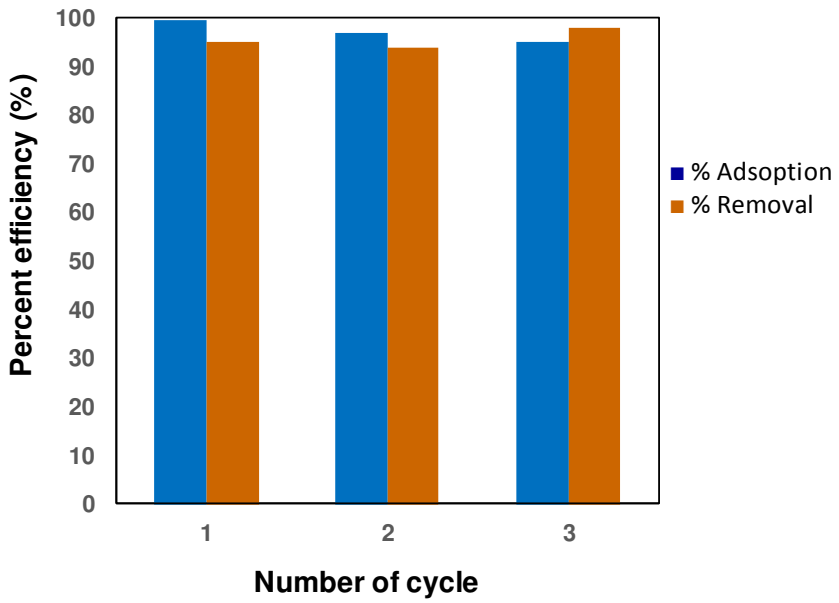

Fig. 11. Adsorption/desorption with repeated cycles on resin **4**.

[Experimental conditions: (i) Adsorption: amount of resin: 20 mg, volume of medium: 40 mL, temperature: 298 K, initial concentration of Cr(III): 1.0 ppm, initial pH: 5.0, (ii) Desorption 0.1 M HNO_3].

3.5. Immobilization mechanism

The adsorption capacities of Cr(III) is increases with increasing pH values in the range 3.0–7.0. The chelating functionality of aminopropylphosphonate may act as a tridentate ligand as depicted in **B** [56,57] in Fig. 12. While the dye is soluble in water, it can also display hydrophobic interaction because of the organic skeleton. The adsorption of MB, as well as the other dyes tested, may well be augmented *via* hydrophobic interaction and π–π stacking as depicted in **C** (Fig. 12) [58]. Owing to resonance, the highly dispersed positive charge in MB is expected to have weak ionic/electrostatic interaction with anionic $-PO_3H^-$ motifs in the resin. Note that zwitterionic motifs are prevalent in resin **4**; as such it can exert electrostatic attraction as well as H-bonding interactions to dyes of both algebraic signs The resin/dye interaction is expected to be a physical adsorption process. After washing with acetone, the dye was removed from the dye-loaded resin, and the colored resin returned back to its original color (Fig. 10). The

regenerated resin was found to be spectrally (FTIR) similar to the original sample, while the regenerated dye remained stable as evinced by UV-Vis spectroscopic analysis.

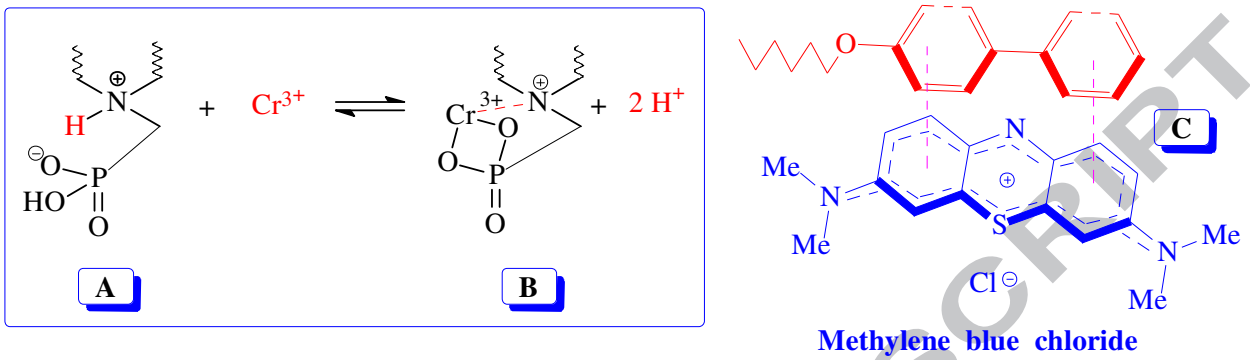

Fig. 12. Aminopropylphosphonate as a chelating ligand to Cr(III) and π-π stacking between methylene blue and p-phenylphenoxy pendant.

4. Conclusions

We have reported on the synthesis, chemical, morphological and thermal evaluation of a novel resin. The resin is synthesized using one-step polymerization of monomers **1**, **2** and cross-linker **3**; the monomers are synthesized in excellent yields from readily available starting materials [31-33]. We reported on the investigation of its adsorption potential in simultaneous exclusion of Cr(III) ions and dyes including methyl orange, Eriochrome black T, rhodamine B, methyl red and methylene blue from aqueous media. The resin showed excellent adsorption performance with high Langmuir monolayer capacity at pH 5. The dosage, temperature, and pH, as well as the surface active sites all, contribute to adsorption efficiency. The regeneration tests were achieved efficiently by using 0.1 M HNO_3 for Cr(III). The reported resin is remarkably successful in removing metal ions including arsenic and dyes from industrial wastewater.

Acknowledgments

The authors would like to acknowledge the support and fund provided by King Fahd University of Petroleum & Minerals (KFUPM) through Project No. IN131053 under the Deanship of Research.

References

[1] L.D. Mafu, T.M. Msagati, B.B. Mamba, Adsorption studies for the simultaneous removal of arsenic and selenium using naturally prepared adsorbent materials, Int. J. Environ. Sci. Technol. 11 (2013) 1723–1732.

[2] D. Mohan, C.U. Pittman, Arsenic removal from water/wastewater using adsorbents-- A critical review, J. Hazard. Mat. 142 (2007) 1–53.

[3] B. Ergül, N. Bektaş, M.S. Öncel, The Use of Manganese Oxide Minerals for the Removal Arsenic and Selenium Anions from Aqueous Solutions, Energ. Environ. Eng. 2 (2014) 103–112.

[4] P. Mondal, C.B. Majumder, B. Mohanty, Laboratory based approaches for arsenic remediation from contaminated water: recent developments, J. Hazard. Mat. 137 (2006) 464–79.

[5] M. Barwick, W. Maher, Biotransference and biomagnification of selenium copper, cadmium, zinc, arsenic and lead in a temperate seagrass ecosystem from Lake Macquarie Estuary, NSW, Australia, Mar. Environ. Res. 56 (2003) 471-502.

[6] T.A. Saleh, Mercury sorption by silica/carbon nanotubes and silica/activated carbon: a comparison study, J. Water Supply Res. T. 64 (2015) 892-903.

[7] H. Saitúa, M. Campderrós, S. Cerutti, A. P. Padilla, Effect of operating conditions in removal of arsenic from water by nanofiltration membrane, Desalination 172 (2005) 173-180.

[8] T.R. Harper, N.W. Kingham, Removal of arsenic from wastewater using chemical precipitation methods, Water Environ. Res. 64 (1992) 200-203.

[9] S. Song, A. Lopez-Valdivieso, D.J. Hernandez-Campos, C. Peng, M.G. Monroy-Fernandez, I. Razo-Soto, Arsenic removal from high-arsenic water by enhanced coagulation with ferric ions and coarse calcite, Water Res. 40 (2006) 364-372.

[10] P. R. Kumar, S. Chaudhari, K.C. Khilar, S.P. Mahajan, Removal of arsenic from water by electrocoagulation, Chemosphere 55 (2004) 1245-1252.

[11] X. Meng, G.P. Korfiatis, C. Christodoulatos, S. Bang, Treatment of arsenic in Bangladesh well water using a household co-precipitation and filtration system, Water Res. 35 (2001) 2805-2810.

[12] T.M. Suzuki, M.L. Tanco, D.A. Pacheco Tanaka, H. Matsunaga, T. Yokoyama, Adsorption characteristics and removal of oxo-anions of arsenic and selenium on the

porous polymers loaded with monoclinic hydrous zirconium oxide, Separ. Sci. Technol. 36 (2001) 103-111.

[13] B. Samiey, C.-H. Cheng, J. Wu, Organic-Inorganic Hybrid Polymers as Adsorbents for Removal of Heavy Metal Ions from Solutions: A Review, Materials 7 (2014) 673-726.

[14] G.J. Alaerts, P. Kelderman, Use of coconut shell-based activated carbon for chromium (III) removal, Water Sci Technol. 21 (1989) 1701–1704.

[15] F. Kanwal, M. Imran, L. Mitu, Z. Rashid, H. Razzaq, Q. Ain, Removal of Chromium(III) Using Synthetic Polymers, Copolymers and their Sulfonated Derivatives as Adsorbents, E-Journal of Chemistry, 9 (2012), 621-630.

[16] M. Rafatullah, O. Sulaiman, R. Hashim, A. Ahmad, Adsorption of methylene blue on low-cost adsorbents: a review, J. Hazard. Mater. 177 (2010) 70-80.

[17] P. Liu, L.X. Zhang, Adsorption of dyes from aqueous solutions or suspensions with clay nano-adsorbents, Sep. Purif. Technol, 58 (2007) 32-39.

[18] S. Kabiri, D.N.H. Tran, M. A. Cole, D. Losic, Functionalized three-dimensional (3D) graphene composite for high efficiency removal of mercury, Environ. Sci.:Water Res. Technol. 2 (2016) 390-402.

[19] L.M. Cui, X.Y. Guo, Q. Wei, Y.G. Wang, L. Gao, L.G. Yan, T. Yan, B. Du, Removal of mercury and methylene blue from aqueous solution by xanthate functionalized magnetic graphene oxide: Sorption kinetic and uptake mechanism, J. Colloid Interf. Sci. 439 (2015) 112-120.

[20] A. Mehdinia, M. Akbari, T.B. Kayyal, M. Azad, High-efficient mercury removal from environmental water samples using di-thio grafted on magnetic mesoporous silica nanoparticles, Environ. Sci. Pollut. Res. 22 (2015), 2155-2165.

[21] T.A. Saleh, Isotherm, kinetic, and thermodynamic studies on Hg (II) adsorption from aqueous solution by silica-multiwall carbon nanotubes, Environ. Sci. Pollut. Res. 22 (2015), 16721-16731.

[22] Y.F. Guo, J. Deng, J.Y. Zhu, C. Zhou, C.Y. Zhou, X.J. Zhou, R.B. Bai, Removal of anionic azo dye from water with activated graphene oxide: kinetic, equilibrium and thermodynamic modeling, RSC Adv. 6 (2016), 39762-39773.

[23] T.A. Saleh, A. Sarı, M. Tuzen, Effective adsorption of antimony (III) from aqueous solutions by polyamide-graphene composite as a novel adsorbent, Chem. Eng. J. 307 (2017) 230-238.

[24] B. Henriques, G. Goncalves, N. Emami, E. Pereira, M. Vila, P. Marques, Optimized graphene oxide foam with enhanced performance and high selectivity for mercury removal from water, J. Hazard. Mater. 301 (2016) 453-461.

[25] Y. K. Zhang, T. Yan, L. G. Yan, X.Y. Guo, L.M. Cui, Q. Wei, B. Du, Preparation of novel cobalt ferrite/chitosan grafted with graphene composite as effective adsorbents for mercury ions, J. Mol. Liq. 198 (2014) 381-387.

[26] J.-H. Deng, X. -R. Zhang, G. -M. Zeng, J.-L. Gong, Q.-Y. Niu, J. Liang, Simultaneous removal of Cd(II) and ionic dyes from aqueous solution using magnetic graphene oxide nanocomposite as an adsorbent, Chem. Eng. J. 226, (2013), 189-200.

[27] G. Z. Kyzas, P. I. Siafaka, E. G. Pavlidou, K. J. Chrissafis, D. N. Bikiaris, Synthesis and adsorption application of succinyl-grafted chitosan for the simultaneous removal of zinc and cationic dye from binary hazardous mixtures, Chem. Eng. J. 259 (2015) 438-448.

[28] S.D. Alexandratos, Ion-Exchange Resins: A Retrospective from Industrial and Engineering Chemistry Research, Ind. Eng. Chem. Res. 48 (2009) 388–398.

[29] A. Deepatana, M. Valix, Recovery of nickel and cobalt from organic acid complexes: adsorption mechanisms of metal-organic complexes onto aminophosphonate chelating resin, J. Hazard. Mater. 137 (2006) 925-33.

[30] S.A. Ali, I.W. Kazi, N. Ullah, A New Chelating Ion-Exchange Resin Synthesized via Cyclopolymerization Protocol and its Uptake Performance for Metal Ions Removal, Ind. Eng. Chem. Res. 54 (2015) 9689–9698.

[31] K. Riedelsberger, W. Jaeger, Polymeric aminomethylphosphonic acids-1. Synthesis and properties in solution, Des. Monomers Polym. 1 (1998) 387–407.

[32] S.A. Ali, S. Z. Ahmed, Z. Hamad, Cyclopolymerization studies of diallyl- and tetraallylpiperazinium salts, J. Appl. Polym. Sci. 61 (1996) 1077-1085.

[33] A. Yamaguchi, A. Yoshizawa, Phase Transition Behaviour of amphiphilic supermolecules possessing a semiperfluorinated alkyl chain, Mol. Cryst. Liq. Cryst. 479, 181–189, 2007.

[34] S. Kudaibergenov, W. Jaeger, A. Laschewsky, Polymeric Betaines: Synthesis, Characterization and Application, Adv. Polym. Sci. 201 (2006) 157-224.

[35] G.B. Butler, Cyclopolymerization and cyclocopolymerization, *Marcel Dekker, New York*, 1992.

[36] H. Martínez-Tapia, Synthesis and Structure of $Na_2[(HO_3PCH_2)_3NH]1.5H_2O$: The First Alkaline Triphosphonate, J. Solid State Chem. 151 (2000) 122-129.

[37] V.C.G.D. Santos, Highly improved chromium (III) uptake capacity in modified sugarcane bagasse using different chemical treatments, Quím. Nova. 35 (2012) 1606-1611.

[38] J. Ščančar, Milačič R., A critical overview of Cr speciation analysis based on high performance liquid chromatography and spectrometric techniques, J. Analyt. Atomic Spectrom. 29 (2014) 427-443.

[39] S. Lagergren, About the theory of so-called adsorption of solution substances, K. Sven. Vetenskapsakad. Handl. 24 (1898) 1-39.

[40] Y.S. Ho, G. McKay, Sorption of dye from aqueous solution by peat, Chem. Eng. J. 70 (1998) 115-124.

[41] W.J. Weber Jr., J.C. Morris, Kinetics of adsorption on carbon from solution, J. Sanit. Eng. Div. Proceed. Am. Soc. Civil Eng. 89 (1963) 31–59.

[42] I. Langmuir, The adsorption of gases on plane surfaces of glass, mica and platinum, J. Am. Chem. Soc. 40 (1918) 1362-1403.

[43] T.W. Weber, R. K. Chakravorti, Pore and solid diffusion models for fixed-bed adsorbers, AIChE J. 20 (1974) 228-238.

[44] H.M.F. Freundlich, Over the Adsorption in Solution, J. Physic. Chem. 57, (1906) 385-471.

[45] M.I. Tempkin, V. Pyzhev, Kinetics of ammonia synthesis on promoted iron catalyst, Acta Phys. Chim. USSR, 12 (1940) 327–356.

[46] S. K. Sahni, R. V. Bennekom, J. A. Reedijk, A spectral study of transition-metal complexes on a chelating ion-exchange resin containing aminophosphonic acid groups, Polyhedron 4 (1985) 1643-1658.

[47] F.C. Wu, R.L. Tseng, R.S. Juang, Initial behavior of intraparticle diffusion model used in the description of adsorption kinetics, Chem. Eng. J. 153 (2009) 1–8.

[48] S. Kocaoba, G. Akcin, Removal and Recovery of Chromium and Chromium Speciation with MINTEQA2, Talanta 57 (2002) 23-30.

[49] F. Gode and E. Pehlivan, Removal of Chromium (III) from Aqueous Solutions Using Lewatit S 100: The Effect of pH, Time, Metal Concentration and Temperature, J. Hazard. Mater. 136 (2006) 330-337.

[50] S. Kocaoba and G. Akcin, Removal of Chromium(III) and Cadmium(II) from Aqueous Solutions, Desalination 180 (2005) 151-156.

[51] S. Kocaoba and G. Akcin, Removal and Recovery of Chromium and Chromium Speciation with MINTEQA2, Talanta 57 (2002) 23-30.

[52] G.J. Alaerts, V. Jitjaturunt, P. Kelderman Use of coconut shell-based activated carbon for chromium(VI) removal, Water Sci. Technol. 21 (1989) 1701-1704.

[53] F. Kanwal, M. Imran, L. Mitu, Z. Rashid, H. Razzaq , Q. Ain, Removal of Chromium(III) Using Synthetic Polymers, Copolymers and their Sulfonated Derivatives as Adsorbents, E-Journal of Chemistry 9 (2012) 621-630.

[54] D. Kolodynska, Z. Hubicki and S. Pasieczna-Patkowska, FT-IR/PAS Studies of Cu(II)–EDTA Complexes Sorption on the Chelating Ion Exchangers, Acta Phys. Pol. A 116 (2009) 340–343.

[55] J. Sheals, P. Persson and B. Hedman, IR and EXAFS Spectroscopic studies of glyphosate protonation and copper(II) complexes of glyphosate in aqueous solution, Inorg. Chem. 40 (2001) 4302-4309.

[56] D. Kołodynska, Z. Hubicki, M. Geca, Application of a New-Generation Complexing Agent in Removal of Heavy Metal Ions from Aqueous Solutions, Ind. Eng. Chem. Res. 47 (2008) 3192-3199.

[57] T.A. Saleh, A.M. Muhammad, S.A. Ali, Synthesis of hydrophobic cross-linked polyzwitterionic acid for simultaneous sorption of Eriochrome black T and chromium ions from binary hazardous waters, J. colloid interf. Sci. 468 (2016) 324-333.

[58] X. He, K.B. Male, P.N. Nesterenko, D. Brabazon, B. Paull, and J.H.T. Luong, Adsorption and Desorption of Methylene Blue on Porous Carbon Monoliths and Nanocrystalline Cellulose, ACS Appl. Mater. Interfaces 5 (2013) 8796–8804.

Highlights

1- A novel resin embedded with metal chelating aminophosphonate was synthesized.

2- The resin imparted remarkable efficacy to remove Cr(III) and dyes simultaneously.

3- The resin showed excellent ability to remove various metals and dyes from wastewater.

.

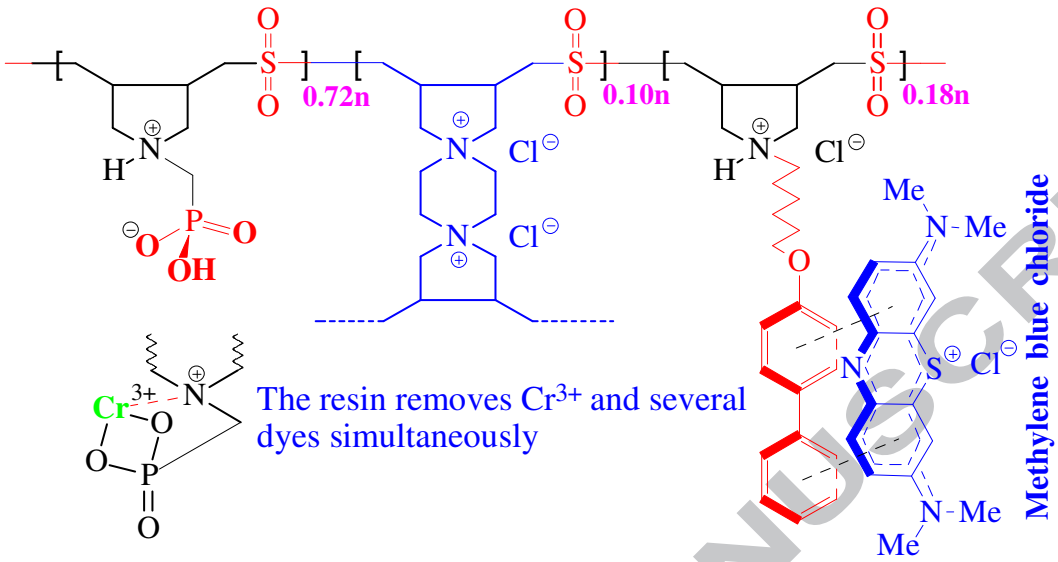

Simultaneous removal metal ions and dyes from industrial wastewater